Modeling of Solidification Conditions and Melt Treatment on Microporosity Formation

K.DAVAMI, M.K.BESHARATY
Department of Mechanical Engineering
University of Tehran
Tehran, Iran P.O Box:11365-4563
IRAN

Abstract : Cast Aluminum-Silicon alloys are used in automotive and industrial weight sensitive applications because of their low density and excellent castability. The presence of trapped gas and or shrinkage pores in certain locations within casting has been shown to influence mechanical properties such as tensile strength and fatigue life. These micromechanical defects can be found most anywhere in casting depending on processing conditions. A large amount of porosity located in the center of the casting may have no effect on mechanical properties or fatigue performance. A smaller, isolated pore near a surface may have significant impact on mechanical properties. Hence , it is important to develop a comprehensive model to predict size, location and distribution of microporosity in casting.
In this work, we model the effect of various casting process parameters on microporosity formation for equiaxed aluminum A356 alloy casting. The process parameters Include cooling rate, grain refiner and eutectic modifier melt additions. The comparisons between experimental results and simulations demonstrate good agreement.

Key-Words: Microporosity; Cooling rate; Grain refiner; Eutectic modifier; Grain nucleation

1 Introduction

The basic principles behind casting processes are straight forward. Molten metal of sufficiently low viscosity flows into cavities of shape complexity, and solidifies upon cooling. However, behind this simple principle lies many complicated reactions and phase transformations. If proper care is not taken, metal casting are prone to defects such as misruns , macroshrinkage (macroporosity), microporosity, segregation, hot tear and residual stress. According to some estimates, the scrap due to casting defects in the U.S alone amounts to approximately 1 billion dollar per year [1]. The design objective of contemporary foundry engineers is to choose an optimized geometry and process parameters that eliminate or minimize defect evolution while ensuring the desired microstructure.

1.1 Effects of eutectic modifiers and grain refiners on microporosity formation

1.1.1 Eutectic Modifiers

Aluminium alloys with silicon as the major alloying addition are used widely by the industry. However ,the presence of brittle , acicular silicon phase in microstructure shows negative effects on mechanical properties of casting. It is because of the brittle nature of the large silicon plates [1] and the sharp edges of the coarse acicular silicon phase promotes crack initiation and propagation[2].The eutectic can be refined by an alloying process known as modification. For aluminium-silicon alloys, this usually involves the addition of strontium (Sr) or sodium (Na) into the melt. Through modification, the acicular silicon is transformed to a fine fibrous structure. Figure 1 and figure 2 show the microstructure of unmodified and modified A356 alloys, respectively. The refinement of Si particle shape improves the mechanical properties of the castings [3,4].However; it is generally observed that modified castings contain more porosity than unmodified ones. The advantage of improving the mechanical properties of the casting can thus be

offset by increased porosity defects[3,4].The increased porosity can have adverse effect on the fatigue properties of casting depending on size and location with respect to free surface[5,6]. Many experiments have been carried out to study and

Table 1: Study of the effect of Na or Sr on Microporosity for Al-Si Alloys

Name	Modifiers	Observation
H.Shahani 1985, [9]	Sr Na	-reduced the gas content but increased porosity -reduced surface tension or acting as nucleants -modifiers promote shrinkage porosity
J.R.Denton J.A.Spittle 1985,[10]	Sr Na	-Sr enhanced the hydrogen susceptibility - Sr enhanced H susceptibility more than Na
D.Argo J.E.Gruzleski 1988,[3]	Sr	- Microshrinkage pores are widely dispersed -larger and slightly increased - Sr increase freezing range
Q.T.Fang D.A.Granger 1989,[14]	Sr	-Sr increased volume fraction of porosity - Sr increases freezing range ,reduces the surface tension and acting as inclusion -increased pore size and pore number density
H.Iwahori et al 1990,[18]	Sr Na	-modifiers increase hydrogen content in the melt -oxide inclusions reduce the rate of degassing and facilitate pore formation -porosity occurs at a lower hydrogen content
K.Tynelius et al 1992,[19]	Sr	-Sr increases area percent porosity -Sr decreases threshold hydrogen limit
D.Emadi et al 1993,[20]	Sr	-Sr or Na decreases surface tension -Sr or Na increases volume shrinkage
A.M.Samuel F.H.Samuel	Sr	-Sr increases areal pore density significantly -pores are mostly round

1995,[21]		-Sr increases pore volume fraction and pore size
N.Roy et al 1996,[11]	Sr	-The increase of pore density and size depends on Sr contents in the melt -A 185 ppm Sr may be approximately equivalent to 0.1 ml/100mg of hydrogen on the effect of porosity
D.Emadi Et al 1996,[10]	Sr	-Hydrogen content remains constant -Sr decreases hydrogen solubility in liquid metal -Hydrogen Solubility in the solid remains constant
J.M.Kim et al 1996,[8]	Sr	-Sr greatly improves feedability Combination of grain refinement and modification reduces shrinkage porosity extremely

explain the effect of eutectic modifiers on hydrogen and microporosity[7,8]. A summary of these findings is shown in Table1.

1.1.2 Grain Refiners

Fine grain structure can be achieved by increasing cooling rate of the casting. Another common practice in industry is to add small amounts of master alloys of Al-Ti, Al-Ti-C or Al-Ti-B to the melt before casting to promote further refinement.

The mechanism of grain refinement is believed to be that numerous potent heterogeneous nucleation nuclei are dispersed in the melt and a large number of these particles act as nucleation sites for the formation of aluminium dendrites. Hence, grain refiner promotes a uniform and equiaxed grain structure [11, 12].It is agreed that when master alloys are added, different intermetallic particles ($TiAl_3, TiB_2, (Al,Ti)B_2, TiC$ or AlB_2) are released into the melt to subsequently act as nucleants. However, the actual physical mechanisms remain unclear. Many experimental studies have been made to observe the effect of grain refiner on porosity[13]. In general, it is observed that the addition of grain refiner increase the grain nucleation sites, thus reducing grain size. This phenomenon leads to the decreasing of the maximum pore size[11].Fang and Granger[14] showed that grain refinement reduced both volume fraction of porosity and pore size in A356.The distribution of porosity was more uniform when grain refiner added. This observation was confirmed by Laorchan *et al.* [25], Kim *et al.*[8]and Roy *et al.*[16].According to Kim *et al.*[18],there are two possible reasons for the reduction of porosity. First, it is possible that mass feeding is improved by this treatment. Another possibility is that the localized feeding distance among solidifying grains is reduced when the number of grain is increased.From these contradictory observations, the only conclusion that can be made is that the addition of TiB_2 will result in more uniform distribution of pores of typically smaller size.

2. Modeling of solidification conditions and melt treatment on microporosity formation

2.1 Cooling rate

Cooling rate plays an important role in determining the microstructure of casting. Higher cooling rate reduces solidification time and grain size of the casting. Hence grain density increases with cooling rate [14, 22]. From experimental observation the

average pore size decreases with increased cooling rate. There are a number of explanations for this phenomena. For a higher cooling rate, the dendrite arm spacing (DAS) decreases as do intergranular regions[14,22].Pore growth is thus limited. Another explanation is that with decreased solidification time, there is less time for hydrogen to diffuse from the solidifying dendrite to the liquid. Hence gas pore growth rate is inhibited.

2.2 Modifier

Eutecitc modifiers are usually added to molten aluminium-silicon alloys to refine the eutectic phase particle shape and improve the mechanical properties of the final cast products[21,23].For aluminium-silicon alloys ,this usually involves the addition of strontium(Sr) or sodium(Na).In general, it is observed that modified casting contain more porosity than unmodified casting. Some possible reasons have been proposed and studied. In general can:

- increase inclusion content in the melt
- decrease hydrogen solubility in solid metal
- change the solid/liquid interface morphology
- reduce surface tension of liquid metal
- increase the volumetric shrinkage

2.3Grain refiner

The effects of grain refiners on porosity are still under study. In general, it is observed that the addition of grain refiners increase the number of grain nucleation sites, thus educing grain size. It has been shown that grain refinement reduces both volume fraction of porosity and pore size in A 356[14]. In addition, distribution of porosity has been found to be more uniform when grain refiner is added [25].

3. Model formulation

In this section, the grain structure evolution model will be presented. The model of gas pore evolution is then described. Finally, the technique for coupling these two models is illustrated in detail.

3.1 Grain structure evolution modelling

Grain nucleation and growth are two phenomena that influence microstructure evolution during the solidification of a casting. In this research, we will model heterogeneous nucleation and growth, a reasonable assumption for commercial casting [24].

3.1.1Grain nucleation

To model heterogeneous nucleation in solidifying casting, two methods have been proposed: an instantaneous model and a continuous model. The instantaneous model assumes all nuclei are formed at a given undercooling temperature. The continuous model assumes nucleation will occur continuously between the equilibrium temperature (i.e. as the liquid undercools), and the maximum undercooling temperature. Due to its simplicity in program implementation, an instantaneous nucleation model is employed in the present study. Using this method, the grain density at a given location can be determined by correlation with the cooling rate, R:

$$N = k_1 + k_2 R + k_3 R^2 \qquad (1)$$

Where k_1, k_2 and k_3 are parameters that need to be determined by empirical analysis of cooling rate and grain size in real casting. Processing conditions such as the addition of grain refiner, eutectic modifiers, and inclusion content, are known to influence the relationship between grain density and cooling rate.

3.2.1 Dendrite growth and orientation

There is a preferred crystallographic orientation for each grain. In our model, each equiaxed grain nucleated in the bulk of the casting is given a principal growth direction, a random positive integer with uniform distribution between 1 and 48. Each integer corresponds to a defined crystallographic orientation in two dimensions.

Rappaz and Gandin[25] have shown that for most metallic alloys, when solidified under normal conditions, the dendrite growth kinetics can be calculated with the aid of the Kurz –Giovanola-Trivedi(KGT) model[26,27].the relationship between dendrite tip velocity and undercooling temperature for Al-7%Su alloy calculated by a KGT model is shown in figure 3.

In general, the probabilistic modelling approach [28] to simulate dendrite growth uses a Cellular Automation (CA) technique [25].With this approach, an individual control volume is divided into uniform cells. Each cell is characterized by different variables, i.e. temperature and states,

liquid, solid or void. An integer is used to record the state of a cell, zero for liquid, negative void and positive for solid. The rules of transition, i.e liquid to solid or liquid to void, of a given cell during one time step are defined according to the states of the neighbouring cells. If a liquid cell is solidified by dendrite growth, it is given the same index as the parent cell.

In our model, a 2-D grid is generated from a given location in the casting where the microstructure and porosity prediction are of interest. The site of the grid scales directly from the computational elements used in macroscopic simulation. The element size of the grid in general is much finer than that of the control volume or element size used in macroscopic heat transfer calculation. The 3-D heat transfer calculation result, such as temperature and solid fraction, for each control volume is then mapped to a grid 2-D grid. The isothermal condition in every element is assumed, so the temperature profiles of an element are applied uniformly to its cells. It is assumed that the microstructure evolution does not influence the local thermal parameters. While such an assumption may not reflect the physical reality, it is a necessary assumption in order to apply a 2-D model to a 3-D process.

3.2 Gas pore evolution modelling

The conditions for a gas pore to grow the solidifying melt is that the gas pressure, P_g, has to be equal or greater than a critical pressure, P_C:

$$P_g \geq P_c \qquad (2)$$

The critical pressure is defined as

$$P_C = P_a + \rho_L gh + P_S + P_\sigma \qquad (3)$$

Where P_a, $\rho_L gh$, P_S and P_σ are the ambient pressure, metallostatic pressure, shrinkage pressure and surface tension per unit area between gas and liquid, respectively. P_a and $\rho_L gh$ are usually constants. P_g and P_s can be calculated , as shown below. Assuming the pore is circular and the surface tension per unit area between gas and liquid is isotropic, P_σ, is given by the well known equation:

$$P_\sigma = \frac{2\sigma_{LG}}{r} \qquad (4)$$

Where σ_{LG} the surface tension between gas and liquid, and r is is the radius of the pore [29].

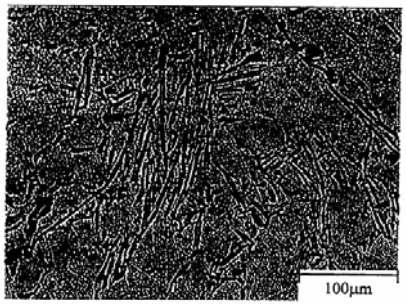

Figure 1: Typical microstructure of unmodified A356 alloy

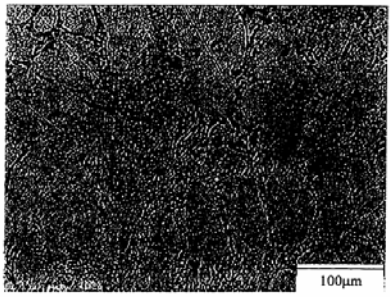

Figure 2 : Typical microstructure of Sr modified A356 alloy

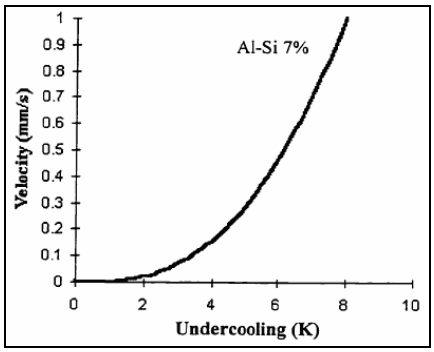

Figure3: Dendrite tip velocity as a function of undercooling for A356 calculated by KGT model

3.2.1 Computation of gas pressure

In most mathematical models for aluminium alloys [30,31], it is assumed that the hydrogen concentrations in liquid and solid at the solidification temperature are in equilibrium. To verify this assumption, the hydrogen diffusivity was calculated and dendrite arm spacing of the

specimen observed. The diffusivity of hydrogen, D (cm/sec), in solid aluminium is given as [32]

$$D = 0.11\exp(\frac{-110950}{RT}) \quad (5)$$

Where R is the ideal gas constant ($\frac{j}{molk}$). From equation 5, at T=823K, D=$1\times10^{-8}\ \frac{cm}{s}$ .The diffusion distance, lambda, is defined as:

$$\lambda = \sqrt{2D\tau} \quad (6)$$

Where τ is the diffusion time. Given the diffusion time, the diffusion distance can be calculated from the Equations 5 and 6. For a permanent mold gravity casting, the solidification time is on the order of 5-10 second. Therefore diffusion distance is about 5 μm.

The size of the dendrite arm for a A356 casting specimen used in this study (to be discussed)is shown in figure 4.It can be seen that the size for half of the dendrite arm is approximately 10 μm.Since the diffusion distance and size of dendrite arm are of the same order, the hydrogen atoms can be assumed to have enough time to diffuse from solid to liquid in permanent mold Al alloy casting used in this study.

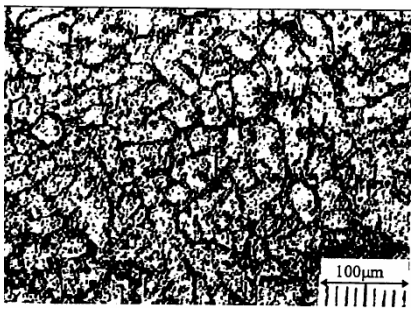

Figure4: Size of dendrite arms for A356 casting specimens

The complete equilibrium condition leads to:

$$\frac{[H_L]}{K_L} = \frac{[H_S]}{K_S} \quad (7)$$

Where $[H_L]$ and $[H_S]$ are the hydrogen concentrations in the liquid and solid metal, respectively, K_L and K_s are constants described below.

Before the formation of gas pore, the hydrogen mass balance equation is given as:

$$(1-f_s)[H_L] + f_s[H_S] = [H_0] \quad (8)$$

Where f_s is solid fraction, $[H_0]$ is the initial hydrogen content in the melt. In addition, The mass concentration of hydrogen dissolved in solid and liquid metal is governed by Sievert`s law.

$$[H_S] = K_S P_g^{1/2} and [H_L] = K_L P_g^{1/2} \quad (9)$$

Which yields Equation 7 for equilibrium conditions.

Combining Equations 8 and 9, the gas pressure before gas pore formation can be calculated as:

$$P_g = (\frac{1}{K_s^{\,2}})(\frac{[H_0]^2}{\left[(\frac{K_L}{K_S}) - (\frac{K_L}{K_S} - 1) f_s\right]^2} \quad (10)$$

The gas pressure increased as solidification proceeds. From Equation 10 , the maximum pressure can be computes as :

$$P_{g,\max} = \frac{[H_0]^2}{K_S^{\,2}} \quad (11)$$

Following classical nucleation theory [29],no gas pore will form if the maximum gas pressure , $P_{g,\max}$ is less than the critical pressure, P_c.Combining Equations 3 and 11 allow us to approximate the critical initial hydrogen content, $[H_0]_C$,above which gas pore can form in the melt. From Equation 3, $P_c \approx 2.75$ atm. If we assume P_a =1atm, h=0.2m , σ_{LG} =0.79N/m[20] , r=10 μm and the negative shrinkage pressure is neglected. Thus,

$$\frac{[H_0]^2}{K_S^{\,2}} = P_C \quad (12)$$

that is,

$$[H_0]_C = K_S\sqrt{P_C} \qquad (13)$$

In this case, when K_s =0.062 $\frac{ml}{100g * atm^{1/2}}$

And P_c =2.75 atm., then $[H_0]_C = 0.10ml/100g$ .It should ne noted that the critical initial hydrogen content depends on many factors such as alloy composition, solidification condition, etc. As such , the above approximation provides an indication of the relationship between initial hydrogen content in the melt and the critical pressure.

When the initial hydrogen content is greater than the critical hydrogen content, gas pressure will form at the critical solid fraction, during solidification. From Equations 8 and 9, the critical solid fraction can be found as:

$$f_c = \frac{\frac{K_L}{K_S} - \frac{[H_0]}{K_s\sqrt{P_c}}}{(\frac{K_L}{K_s} - 1)} \qquad (14)$$

Note that f_c decreases as $[H_0]$increases and P_c decreases.When initial hydrogen content is high, the melt will reach the domain where gas pores will form at an earlier stage of solidification. In addition, the addition of eutectic modifiers in the melt reduces the surface tension of liquid aluminium alloy [20] which results in the reduction of P_c (Equations 3 and 4). Hence, the critical solid fraction is reduced and gas pores can nucleate earlier and grow over a longer period of time.

When gas pore formation condition is satisfied as defined in Equation 2, some hydrogen will be trapped in the gas pore. The hydrogen mass balance equation in this case is given as :(15)

$$[H_0]\rho_L = [H_S]\rho_S f_S + [H_L]\rho_L(1 - f_S - f_\upsilon) + \alpha\frac{f_\upsilon P_g}{T}$$

Where $[H_0]$is the initial hydrogen content in the melt, $[H_s]$and $[H_L]$are the hydrogen contents in the solid and liquid; ρ_L and ρ_s are the densities for liquid and solid metal; f_s and f_υ are the volume fraction of solid and porosity; α is a gas conversion factor[30], P_g is gas pressure; and T is the temperature. The last term in the equation represents the amount of hydrogen trapped in the gas pore. By substituting Equation 9 to Equation 15 , the gas pressure after the gas pore has formed can be computed.

3.2.2 Computation of shrinkage pressure

The shrinkage pressure associated with liquid metal flow in the mushy zone represent the contribution of solidification shrinkage in microporosity formation. To determine the shrinkage pressure, the mass conservation equation must be solved.

$$(\frac{\rho_s}{\rho_L} - 1)\frac{\delta f_s}{\delta t} - \frac{\delta f_v}{\delta t} + div(f_L\bar{u}) = 0 \qquad (16)$$

Where ρ_s and ρ_L are densities of solid and liquid metal, f_s, f_v and f_L are fractions of solid, porosity and liquid, t is time and $\bar{u}$ is the interdendritic flow velocity vector. The first term in Equation 16 represents the volume shrinkage associated with solidification. This shrinkage is compensated by the growth of gas porosity and or by liquid metal feeding. The interdendritic flow velocity, $\bar{u}$,can be calculated by Darcy's law[30,33].

$$\bar{u} = -\frac{K}{\mu f_L}(\nabla P + \rho_L gt) \qquad (17)$$

Where K is the permeability of the medium, μ is viscosity, f_L is volume fraction of liquid, P_s is shrinkage pressure, ρ_L is density of liquid, g is acceleration due to gravity and t is the unit vector along the direction of gravity. The permeability is defined as [30]:

$$K = \frac{{f_L}^3 {d_2}^2}{180(1 - f_L)^2} \qquad (18)$$

Where d_2 is the secondary dendrite arm spacing. The pressure can be calculated by solving the Equations 16-18 simultaneously.

3.2.3Pore formation

Pore formation is a complex phenomenon. For the existing mathematical models, the initial nucleus size is usually assumed to be fraction of the secondary dendrite arm spacing [23,33] or a very small number $(1\ \mu m)$ [14]. In our model, the pore nucleus radius is assumed to be equal to half of the size of the cell $(5\sim10\ \mu m)$.

Equation 2 shows that the gas pore can form only when its pressure is sufficiently large to overcome the total local external pressure. After every term in Equation 2 and 3 is obtained by solving the basic equations, the program then checks and decides whether the pore formation condition is met, i.e gas pressure is greater or equal to the sum of local liquid metal pressure and surface tension. If the condition is satisfied, a gas pore is formed and is stable. The program then randomly selects a liquid cell and assigns it to become a gas pore.

3.2.4 Pore growth

As solidification continues, more hydrogen atoms are rejected from the growing solid into the liquid. If the pressure of dissolved hydrogen is sufficient, the pore can grow.

During each time step, the pressure terms are calculated for every element in the location of interest. The calculation is reported until there are no liquid cells remaining in the elements, i.e. until solidification complete.

3.3 Coupling of grain structure and pore evolution models

In the micro-model, the time step used in the calculation should be determined first. From the KGT model, the dendrite tip velocity V(*mm/s*) is known given a undercooling temperature, Figure 3. With a pre-defined cell size *d*(μm), the time step $\Delta t(s)$ can be calculated:

$$\Delta t = \frac{d}{V} \qquad (19)$$

After the time step is determined, the microstructure prediction model starts with random selection of nucleation sites. The selection are made in every element that is on the two dimensional grid when the element reaches the specified undercooling temperature. The number of nuclei that will form every element is calculated:

$$p = x \times \left(\frac{N}{n} \right) \qquad (20)$$

Where x is a random number that is uniformly distributed between 0 and 1, N is the number of liquid cells available in the element and n is the grain density of the element. A nucleus will form if $p \le 1.0$ .For every element, N , is decreased By one after each iteration. On the other hand, the grain density of the element , n , is decreased by one only when the nucleus is formed(i.e. $p \le 1.0$). A flow chart for this random cell selection process is shown in figure 5.

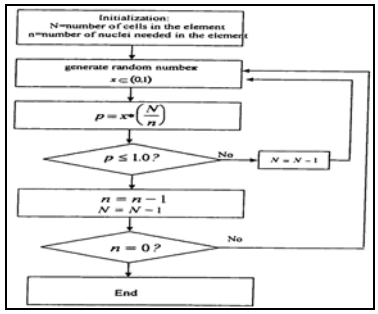

Figure5:Flow chart for grain nucleus selection

In subsequent time steps, equiaxed grain growth is simulated. Since it is assumed that all the nuclei are formed at the same undercooling temperature, the dendrite tip growth velocity will be the same for all nuclei (Figure3).With the number of nuclei in every element determined, one can find the dendrite growth velocity that corresponds to the change of solid fraction calculated by the macro model. After the growth velocity is determined, one needs to choose the time step used in the micro model calculation.

In the micro model, a solid cell grows with square von Neumann nearest-neighbor configuration [25], however, it should be noted that their dendrite tip correction scheme is not incorporated in our model.

From experimental observations, it is known that hydrogen gas pores form in a spherical shape in the melt[34]. The difference in pore shapes depend on whether the pores are able to grow without obstruction or whether they are obstructed to a greater or lesser extent by other dendrites growing in the melt [34,35]. In the simulation when the gas

pore growth condition is satisfied, growth occurs incrementally in steps determined by cell size.

Figure 6 is a schematic for the cellular automation used to simulate gas pore growth in the model. As mentioned before, The radius of the initial gas pore is assumed to be one half of the cell size; this means that gas pore will occupy one cell in he element, as shown in figure 6(a). During the next time step in the micro model, if gas pore has already formed, the program will check the possibility for growth. By assuming that the gas pore grows in increments of half of the cell size, the gas pore will have a radius equal to one cell size. This means that the gas pore will occupy four cells in the element, as shown in figure 6(b). As growth proceeds, the gas pore then has a radius equal to one and half cell sizes. As much, it will occupy nine cells in the element, as shown in figure 6(c) and so on. In this way, gas pores can grow radially(for two dimension)as observed in experiment[34].

If gas pores can not grow radially, i.e. near the end of solidification process when most of the molten metal has solidified, it is assumed that gas pores will expanded to the remaining liquid cells that surround the pores, if any. With this assumption, the expansion of gas pores within a growing dendrite network can be simulated. During the solidification process, shrinkage pores will form because some of the liquid cells will be engulfed by solid. Thereby choking the flow of feeding liquid. In the model, the formation of isolated shrinkage pores is checked after every iteration(figure 7).

With the algorithm described above, a gas pore will be able to grow circularly if it is formed at an early stage of solidification. During this time, the casting is mostly molten metal. There is no difficulty for the gas pore to find the liquid pool that is needed for the pore to grow radially. As solidification progresses , the growth of the gas pore will be influenced by the advancing dendrite network. In the model, when a gas pore can not grow radially, it will expand between the dendrites.

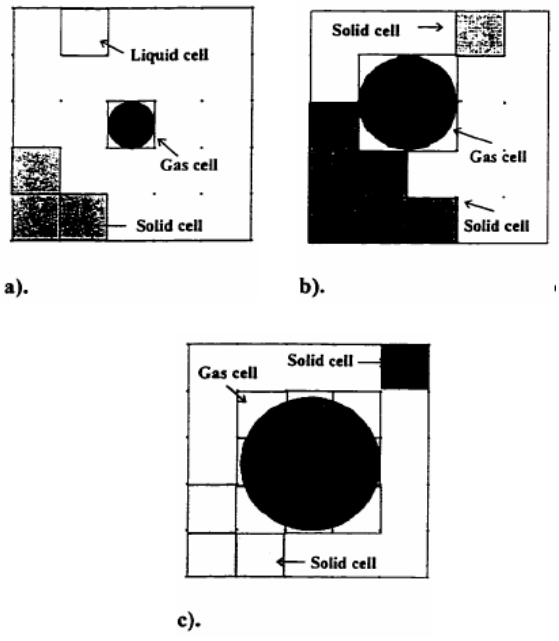

Figure6:Schematic for the cellular automation used to simulate gas pore growth

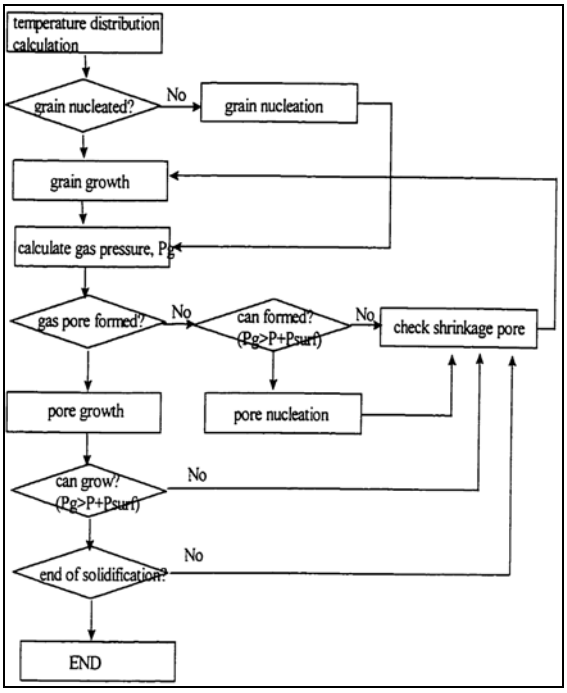

Figure7:Flow chart of the proposed model

4. Conclusions

A two dimensional model to predict pore size, morphology and location has been developed for A356 aluminium alloy solidifying under equiaxed grain structure conditions. To improve upon the conventional deterministic approach, the model links hydrogen gas evolution and microporosity formation mechanisms with a probabilistic grain

structure evolution model with reasonable confidence. This information can then be used to evaluate static and dynamic mechanical performances of casting during the earliest stage of product definition.

The following conclusions are drawn from this study:

1. For a permanent mold, Al alloy casting, the diffusion distance and size of dendrite arm of the same order. Hence, the approximation of complete equilibrium for hydrogen dissolved in solid and liquid can be assumed.

2. As solidification proceeds, no gas pore forms until hydrogen gas pressure reaches a critical value.

3. There exists a critical initial hydrogen content below which gas pore can not form the melt. The critical initial hydrogen content depends on many factors such as alloy composition, solidification condition, etc.

4. When the initial hydrogen content is greater than the critical hydrogen content, gas pores will form at a critical solid fraction during solidification. The critical solid fraction decreases as the initial hydrogen content in the melt decreases and critical pressure decreases.

5. Form experimental observation, the addition of grain refiner, 0.07wt% TiB_2 decreases the grain size, pore area fraction and pore size of the casting. In addition, it is observed that pores are more uniformly distributed.

6. Besides grain refinement, cooling rate has strong influence on the size grains.

References:

[1]I.J. Polmear, Light Alloys, Halsted Press, London , 3rd edition,1995,1995,pp72,pp176.

[2]W.Laorchan, and I.E Gruzleski, "Grain Refinement, Modification and Melt Hydrogen-Their Effects on Microporosity, Shrinkage , and Impact Properties in A356 Alloys", AFS Transactions, 100,1992,pp415-422.

[3]D.Argo and J.E Gruzleski "Porosity in Modified aluminum Alloy Castings" ,AFS Transactions,1988,pp65-74.

[4]A.M Samuel and F.H. Samuel, "Review: Various Aspects Involved in The Production of Low-Hydrogen Aluminum castings" ,Journal of Material Science,27,1992,pp6533-6563.

[5] M.E. Seniw, M.E. Fine, E.Y. Chen,M.Meshii and J.Grazy, "Relationship of Defect Size and location to Fatigue Failure in Al Alloy A356 Cast Specimens",Paul C,paris International Symposium " Fatigue Materials",TMS-ASM Fall meeting,1997.

[6]J.A Eady and D.M. Smith ,"The Effect of Porosity on the Tensile Properties of Aluminum Alloy Casting" Mat.Forum,9(4),1986,pp217-233.

[7]B.Closset and J.E.Gruzleski,"Structure and properties of Hypoeutectic Al-Si-Mg Alloys Modified with Pure Strontium",Met. and mat. Transactions, 13 A,1982,pp945-951.

[8]J.M.Kim, H.W.Kwon, D.G.Kim and C.R. Loper, Jr., :Porosity Formation in Relation to the Feeding Behavior of Al-Si Alloys",101 Casting Congress, American Foundry Society,1997,97-066.

[9]H.Shahani, "Effect of Hydrogen on the Shrinkage Porosity of Aluminum Copper and Aluminum Silicon Alloys" ,Scandinaviam Journal of Metallurgy,14,1985,pp306-312.

[10]D.Emadi, h.Lu, J.E Gruzleski and M.Bouchard, "Effects of Sr-modification on the Melt Hydrogen Content and the Hydrogen Solubility in the Solid and Liquid Al-Si Alloys",Proceedings of the 1996 125th TMS Annual Meeting,1996,pp721-727.

[11]N.Roy, A.M.Samuel, and F.H Samuel, "Porosity Formation in Al-9Wt Pct Si-3Wt Pct Cu AlloysSystems:Metallorgraphic Observations",Met. and Mat.Transactions,27A, 1996,PP415-429.

[12]P.S.Mohanty, F.H.Samuel, J.E. Gruzleski and T.J.Kosto,"Studies on the Mechanism of Grain Refinement in Aluminum",Light etals,1994,pp1039-1045.

[13] P.S.Mohanty and J.E.Gruzleski,"Grain Refinement Mechanisms of Hypoeutectic Al-Si Alloys",Acta.Material,vol.44,No,9,1996,pp3749-3760.

[14]Q.T.Fang and D.A.Granger,"Porosity Formation in Modified and Unmodified A356 Alloy Casting" AFS Transactions,97,1989,pp989-1000.

[15]W.Laorchan, and J.E.Gruzleski, "Grain Refinement, Modification and Melt Hydrogen-Their Effects on Microporosity,Shrinkage, and Impact Properties in A356 Alloy",AFS Transactions,100,1992,pp415-422.

[16]N.Roy,Zhang, P.R.Louchez and F.H.Samuel,"Porosity Formation in Al-9Wt Pct Si-3Wt Pct Cu Alloy SYSTEMS:Measurements of Porosity",Journal of Material Science,31,1996,pp1234-1254.

[17]J.R.Denton and J.A.Spittle, "Solidification and Susceptibility to Hydrogen Absorption of Al-Si Alloys Containing Strontium", Material Science and Technology,1,April,1985,pp305-311.

[18]H.Iwahori,K.Yonekura,Y.Yamamoto, and M.Nakamura, "Occurring Behavior of Porosity and Feeding Capabilities of Sodium and Strontium Modified Al-Si Alloys", AFS Transactions, 98,1990,pp167-173.

[19]K.Tynelius, J.F.Major and D.Apelian, "A Parametric Study of Microporosity in the A356 Casting Alloy System"AFS Transactions,1993,pp401-413.

[20]D.Emadi, J.E.Gruzleski and J.M.Toguri, "The Effect of Na and Sr Modification on Surface Tension and Volumetric Shrinkage of A356 Alloy and Their Influence on Porosity Formation", Met. Trans.B,1993,24B,pp1055-1063.

[21]A.M.Samuel and F.H.Samuel, "Effect of Melt Treatment, Solidification Conditions, and Porosity Level on the Tensile Properties of 319.2EndchillAluminum Castings", Journal of Materials Sicence,30 , 1995,pp4823-4833.

[22]S.Shivakumar, D.Apelian and J.Zou, "Modeling of Microstructure Evolution and Microporosity Formation in Cast Aluminum Alloys" AFS Transactions,98, 1990.pp897-904.

[23]J.E Gruzleski, "The Art and Science of Modification:25 Years of Progress" ,AFS Transactions,92-164,1992,pp673-683.

[24]M.Flemings, Solidification Processing, McGraw-Hill,1974.

[25]M.Rappaz,Ch-A.Gandin, "Probabilistic Modeling of Microstructure Formation in SolidificationProcess",Acta Metallurgica,41,1993,pp345-360.

[26]W.Kurz, B.Giovanola, and R.Trivedi, "Theory of Microstructural Development During Rapid Solidification", Acta Metall.,1986,34,pp823-830.

[27]J.L.Spittle and S.G.R. Brown,"Computer Simulation of the Effect of Alloy Variables on the Grain Structures of Castings", Acta Metallurgica,37,1989,pp1803-1810.

[28]M.Rappaz, "Modelling of Microstructure Formation in Solidification Processes", International Materials Reviews,34.No.3,1989,pp93-123.

[29]M.E.Fine, Introduction to Phase Transformations in Condensed Systems, Macmillan Co.,1964,pp7.

[30]K.Kubo and R.Phelke, "Mathematical Modeling of Porosity Formation Solidification",Met. Transactions B,16B, June 1985,pp359-366.

[31]J.Ampuero, A.F.A. Hoadly, and M rappaz, "Numerical and Experimental Study of Microporosity Evolution During the Solidification of Metallic Alloys", Modeling of Casting, Welding and Solidification Processes,V,1991,PP449-454.

[32]E.A.Brandes and G.B.Brooks(editors), Smithells Metals Reference Book 7th edition,Butterworth-Heinmann,1992,pp13-72.

[33]J.D.Zhu and I.Ohnaka, "Computer Simulation of Interdendritic Porosity in Aluminum Alloy Ingots and Casting", Modeling of Casting, Welding and Solidifications Processes, V,1991,pp435-442.